

# Diffusion and criticality in undoped graphene with resonant scatterers

P. M. Ostrovsky,<sup>1,2</sup> M. Titov,<sup>3,1</sup> S. Bera,<sup>1,4</sup> I. V. Gornyi,<sup>1,5,4</sup> and A. D. Mirlin<sup>1,6,7,4</sup>

<sup>1</sup> *Institut für Nanotechnologie, Karlsruhe Institute of Technology, 76021 Karlsruhe, Germany*

<sup>2</sup> *L. D. Landau Institute for Theoretical Physics RAS, 119334 Moscow, Russia*

<sup>3</sup> *School of Engineering & Physical Sciences, Heriot-Watt University, Edinburgh EH14 4AS, UK*

<sup>4</sup> *DFG Center for Functional Nanostructures, Karlsruhe Institute of Technology, 76128 Karlsruhe, Germany*

<sup>5</sup> *A.F. Ioffe Physico-Technical Institute, 194021 St. Petersburg, Russia.*

<sup>6</sup> *Inst. für Theorie der kondensierten Materie, Karlsruhe Institute of Technology, 76128 Karlsruhe, Germany*

<sup>7</sup> *Petersburg Nuclear Physics Institute, 188300 St. Petersburg, Russia.*

A general theory is developed to describe graphene with arbitrary number of isolated impurities. The theory provides a basis for an efficient numerical analysis of the charge transport and is applied to calculate the minimal conductivity,  $\sigma$ , of graphene with resonant scatterers. In the case of smooth resonant impurities  $\sigma$  grows logarithmically with increasing impurity concentration, in agreement with renormalization group analysis for the symmetry class DIII. For vacancies (or strong on-site potential impurities)  $\sigma$  saturates at a constant value that depends on the vacancy distribution among two sublattices as expected for the symmetry class BDI.

PACS numbers: 73.63.-b, 73.23.-b, 73.22.Pr

Transport properties of graphene [1–3] remain in the focus of intense studies. It has been established, both theoretically [4, 5] and experimentally [6–10], that the conductivity of short and wide samples of ballistic graphene acquires a minimal value of  $4 \times e^2/\pi h$  (the factor 4 reflecting the spin and valley degeneracy) when the chemical potential is tuned to a vicinity of the Dirac point. The minimal conductivity of larger graphene flakes is close to  $4 \times e^2/h$  for the majority of experimentally available samples [2]. The enhancement of the minimal conductivity is attributed to the effect of disorder: graphene near the Dirac point may conduct better when impurities are added [11–13].

Remarkably, the minimal conductivity of disordered graphene remains essentially constant when the temperature  $T$  is lowered by several orders of magnitude, down to 30 mK [14]. This is in contrast with the behavior of conventional 2D systems with conductivity  $\sigma \sim e^2/h$ : their  $\sigma$  gets strongly suppressed with lowering  $T$  due to Anderson localization. The absence of localization in graphene indicates that the dominant disorder is either of long-range character (and thus does not mix the valleys) or preserves a chiral symmetry of the Hamiltonian [15, 17]. The former possibility has been investigated in Refs. [12, 13, 16, 17]. In this paper we explore the case of resonant impurities that preserve the chiral symmetry ( $C_z$  in terminology of Ref. [15]).

Resonant scatterers create “mid-gap” states directly at the Dirac point, thus having a strong impact on the minimal conductivity. A natural example of a resonant scatterer is a strong potential applied to a site of a graphene honeycomb lattice, which is equivalent to a vacancy. In this way, vacancies are effectively created by hydrogen ad-atoms or  $\text{CH}_3$  molecules, which bind to a single carbon atom in graphene and change its hybridization from  $sp^2$  to  $sp^3$  type. The resonant character of hydrogen

ad-atoms was supported by the DFT analysis [18]. Resonant scatterers give linear (up to a logarithmic factor) dependence of the graphene conductivity on electron density [15, 19], consistent with experimental observations. Recent experiments [20, 21] confirmed that a moderate concentration of hydrogen adsorbates preserves all the salient features of transport in graphene and provided evidence that resonant impurities determine the graphene mobility.

The vacancies are not the only type of resonant impurities. For instance, a smooth potential impurity, which can be represented by a scalar potential in the Dirac equation, is resonant provided the energy of the localized impurity state coincides with the Dirac point. Recent works [22, 23] studied the effect of resonant scalar impurities in the ballistic regime. It was shown, in particular, that each such impurity enhances the conductance of ballistic graphene by a value of the order of  $e^2/h$ .

In this Letter we develop a general theory of transport in a system with arbitrary number  $N$  of isolated impurities. The full counting statistics of the system is given by a determinant of a matrix of size  $N$ . The averaging over impurity positions can be performed numerically with a high efficiency. We apply this theory to disordered graphene at the Dirac point, focusing on two types of resonant scatterers: scalar (smooth potential) impurities and vacancies. This allows us to explore the diffusive (or critical) regime that is established with increasing concentration of impurities (or, equivalently, sample length).

We consider a graphene sample of the length  $L$  and the width  $W \gg L$ , which is described by the Dirac Hamiltonian,  $H = -i\hbar v \boldsymbol{\sigma} \nabla + V(\mathbf{r})$ , where  $\boldsymbol{\sigma} = (\sigma_x, \sigma_y)$  is the vector of Pauli matrices,  $v$  is the velocity, and  $V(\mathbf{r})$  is an impurity potential that can mix valleys and sublattices. Hereafter we set  $\hbar v = 1$ .

Metallic leads at  $x < 0$  and  $x > L$  are defined by adding a large chemical potential,  $\mu_\infty \rightarrow \infty$ . Inside the sample, i.e. for  $0 < x < L$ , the chemical potential is tuned to the Dirac point ( $\mu = 0$ ). The function  $V(\mathbf{r}) = \sum_{n=1}^N V_n(\mathbf{r})$  represents  $N$  isolated scatterers.

To calculate the full counting statistics of electron transport we use the matrix Green function approach [23, 24, 27]. The Green function in the retarded-advanced (RA) space satisfies the equation

$$\begin{pmatrix} \mu - H + i0 & -\sigma_x \zeta \delta(x) \\ -\sigma_x \zeta \delta(x - L) & \mu - H - i0 \end{pmatrix} \mathcal{G}(\mathbf{r}, \mathbf{r}') = \delta(\mathbf{r} - \mathbf{r}'), \quad (1)$$

where  $\zeta = \sin(\phi/2)$  is the counting field and the chemical potential  $\mu$  equals  $\mu_\infty$  in the leads and zero in the sample. It is important for the subsequent analysis that the bare Green function  $\mathcal{G}_0$ , which solves Eq. (1) at  $V = 0$ , can be calculated analytically [23].

Transport quantities (conductance, noise, and higher order cumulants) are readily determined from the cumulant generating function  $\mathcal{F} = \text{Tr} \ln \mathcal{G}^{-1}$ , where the trace  $\text{Tr}$  includes the spatial coordinates as well as RA, sublattice, and valley indices. Below we are mostly concerned with the conductance determined by the relation

$$G = -(4e^2/h) (\partial^2 \mathcal{F} / \partial \phi^2)_{\phi=0}. \quad (2)$$

With the help of the Dyson equation,  $\mathcal{G}^{-1} = \mathcal{G}_0^{-1} - V$ , we obtain  $\mathcal{F} = \mathcal{F}_0 + \delta\mathcal{F}$ , where  $\delta\mathcal{F} = \text{Tr} \ln(1 - V\mathcal{G}_0)$  describes the correction to the cumulant generating function,  $\mathcal{F}_0 = \text{Tr} \ln \mathcal{G}_0^{-1} = -W\phi^2/2\pi L$ , of the clean system [23].

Our aim is to take advantage of the fact that impurities do not overlap and to reduce the operator determinant in the definition of  $\delta\mathcal{F}$  to the usual matrix determinant. Such a reduction is justified if the impurity size is smaller than both the distance between impurities and the Fermi wave length (the latter is infinite at the Dirac point). The generating function can be rewritten in the  $N$ -dimensional unfolded (impurity) space as

$$\delta\mathcal{F} = \text{Tr} \ln(1 - V\mathcal{G}_0) = \text{Tr} \ln(1 - \hat{V}\hat{\mathcal{G}}_0), \quad (3)$$

where  $\hat{V} = \text{diag}(V_1, V_2, \dots, V_N)$  and all elements of the matrix  $\hat{\mathcal{G}}_0$  are identical and equal to the operator  $\mathcal{G}_0$ .

We proceed with introducing the  $T$ -matrix operators  $T_n = (1 - V_n g)^{-1} V_n$ , that account for multiple rescattering on individual impurities [23]. Here  $g$  stands for the Green function in an infinite graphene plane. At the Dirac point we find

$$g(\mathbf{r}, \mathbf{r}') = -(i/2\pi) \boldsymbol{\sigma} \cdot (\mathbf{r} - \mathbf{r}') / |\mathbf{r} - \mathbf{r}'|^2. \quad (4)$$

Using the definition of the  $T$ -matrix, we rewrite  $\delta\mathcal{F}$  as

$$\delta\mathcal{F} = \text{Tr} \ln [1 - \hat{T}(\hat{\mathcal{G}}_0 - g)] + \text{Tr} \ln(1 - \hat{V}g), \quad (5)$$

where  $\hat{T} = \text{diag}(T_1, T_2, \dots, T_N)$  and  $g$  is proportional to the unit matrix in the unfolded space.

The last term in Eq. (5) does not depend on the source field,  $\phi$ , and can be safely omitted. Taking the limit of point-like impurity we reduce the operator product in the first term of Eq. (5) to the standard matrix product with the result

$$\delta\mathcal{F} = \text{Tr} \ln(1 - \hat{T}\hat{\mathcal{G}}_{\text{reg}}), \quad (6)$$

where  $\hat{T}$  is the diagonal matrix of integrated impurity  $T$ -matrices (describing  $s$ -wave scattering only) and the elements of the matrix  $\hat{\mathcal{G}}_{\text{reg}}$  in the unfolded space are given by

$$(\hat{\mathcal{G}}_{\text{reg}})_{nm} = \begin{cases} \mathcal{G}_0(\mathbf{r}_n, \mathbf{r}_m), & m \neq n, \\ \lim_{\mathbf{r} \rightarrow \mathbf{r}_n} [\mathcal{G}_0(\mathbf{r}_n, \mathbf{r}) - g(\mathbf{r}_n, \mathbf{r})], & m = n, \end{cases} \quad (7)$$

where  $\mathbf{r}_n = (x_n, y_n)$  specify the positions of impurities.

Equation (6) is one of the central results of the Letter. The impurity-induced correction to the full-counting statistics is reduced to the finite-size matrix determinant, which is completely defined by the impurity  $T$ -matrices in the  $s$ -wave channel and the bare Green function. The  $T$ -matrices can be found in a standard way from the solution of the corresponding single impurity scattering problem [28]. The exact bare Green function in the rectangular geometry of Eq. (1) has been calculated in Ref. [23]. It is given by the matrix product

$$\mathcal{G}_0(\mathbf{r}_n, \mathbf{r}_m) = \frac{i}{4L} U_{x_n} \Lambda \Sigma_z e^{\Sigma_y(y_n - y_m)\phi/2L} R \Lambda U_{x_m}^{-1}, \quad (8)$$

where  $\Sigma_{x,y,z}$  are the Pauli matrices in RA space and

$$U_x = \begin{pmatrix} \sin \frac{\phi(x-L)}{2L} & \cos \frac{\phi(x-L)}{2L} \\ i \cos \frac{\phi x}{2L} & i \sin \frac{\phi x}{2L} \end{pmatrix}_{RA}, \quad \Lambda = \begin{pmatrix} 1 & 0 \\ 0 & \sigma_z \end{pmatrix}_{RA}.$$

The matrix  $R$  is acting in the sublattice space. In the limit  $W \gg L$  it simplifies to

$$R(\mathbf{r}_n, \mathbf{r}_m) = \begin{pmatrix} \csc(z_n + z_m^*) & \csc(z_n - z_m) \\ \csc(z_n^* - z_m^*) & \csc(z_n^* + z_m) \end{pmatrix}_\sigma, \quad (9)$$

where  $z_n = \pi(x_n + iy_n)/2L$  and  $\csc z = 1/\sin z$ . The matrix  $R$  coincides with the retarded Green function of the clean sample up to a factor  $4iL$ .

The expressions (8), (9) define the off-diagonal elements of the matrix  $\hat{\mathcal{G}}_{\text{reg}}$  in the unfolded space. The diagonal elements are found from Eq. (7) as

$$(\hat{\mathcal{G}}_{\text{reg}})_{nn} = \frac{i}{4L} U_{x_n} \Lambda \Sigma_z R_{\text{reg}} \Lambda U_{x_n}^{-1}, \quad (10)$$

where  $R_{\text{reg}}(\mathbf{r}) = \csc(\pi x/L) + \Sigma_y \sigma_y \phi/\pi$ . Diagonal part of the matrix  $R_{\text{reg}}$  is proportional to the local density of states in a clean setup. Equation (10) completes the construction of the matrix  $\hat{\mathcal{G}}_{\text{reg}}$ .

The only input parameters for the general result (6) are  $T$ -matrices of individual impurities. They can be

obtained by solving the single impurity scattering problem. For smooth potential impurity, the  $T$ -matrix mixes neither sublattices nor valleys and is given by the scattering length,  $T = \ell$ . The length  $\ell$  diverges if the impurity potential fulfills the resonant condition [23]. In contrast, the  $T$ -matrix for an on-site potential impurity projects on a one-dimensional subspace,  $T = \ell|u\rangle\langle u| = \ell(1 \mp \tau_x \sigma_x \pm \tau_y \sigma_y + \tau_z \sigma_z)/4$ , where upper (lower) sign correspond to the impurity in A (B) sublattice, respectively, and  $\tau_\alpha$  are the Pauli matrices in the valley space [28]. The vacancy (i.e. infinitely strong on-site potential) corresponds to the limit  $\ell \rightarrow \infty$ .

In general, the  $T$  matrix of a resonant impurity is given by a divergent length scale,  $\ell$ , multiplied by a projection operator acting in the valley and sub-lattice space. This enables further simplification of the result (6) by omitting the unity under the logarithm in the projected basis. Up to an arbitrary constant term, the resulting generating function can be cast in the form

$$\delta\mathcal{F} = \text{Tr} \ln \hat{K} \hat{K}^\dagger, \quad (11)$$

with a matrix  $\hat{K}$  satisfying the identity  $\hat{K}^\dagger(\phi) = \hat{K}(-\phi)$ . For resonant scalar impurities, the elements of  $2N \times 2N$  matrix  $\hat{K}$  are given by

$$K_{nm} = \begin{cases} \sigma_z R(\mathbf{r}_n, \mathbf{r}_m), & m \neq n, \\ \sigma_z \csc(\pi x_n/L) - i\sigma_x \phi/\pi, & m = n. \end{cases} \quad (12)$$

For vacancies, the matrix  $\hat{K} = \hat{A} + \hat{A}^T$  has a dimension  $N \times N$  with

$$A_{nm} = \frac{\exp\left[\frac{\phi}{2L}(y_n - y_m) - \frac{i\pi}{4}(\zeta_n - \zeta_m)\right]}{\sin\left[\frac{\pi}{2L}(\zeta_n x_n + \zeta_m x_m + iy_n - iy_m)\right]}, \quad (13)$$

where  $\zeta_n = \pm 1$  if the  $n$ -th vacancy belongs to the sublattice A (B). The analytical expressions (11)–(13) can now be used for the efficient numerical evaluation of the conductance, noise, and higher transmission cumulants of a disordered graphene sample. Below we focus on the conductance, Eq. (2). In terms of  $\hat{K}$  it is given by

$$G = \frac{4e^2}{\pi h} \left\{ \frac{W}{L} + 2\pi \text{Tr} \left[ (\dot{K} K^{-1})^2 - \ddot{K} K^{-1} \right]_{\phi=0} \right\}, \quad (14)$$

where dots denote derivatives with respect to  $\phi$ . In the case of resonant potential impurities, the matrix  $K$  is linear in  $\phi$ ; hence the last term drops from Eq. (14).

Computational efficiency of Eq. (14) is limited by inverting the matrix  $K$  at  $\phi = 0$ . This operation involves  $O(N^3)$  multiplications. We run the standard matrix-inverse update algorithm by adding impurities one by one to compute the dependence of conductivity on  $N$ . This reduces the complexity to  $O(N^2)$  per realization on average. The procedure is repeated many times to get sufficient statistics for different ratios  $W/L$ . Then we extrapolate the result to the limit  $W \rightarrow \infty$ , thus eliminating non-universal boundary effects.

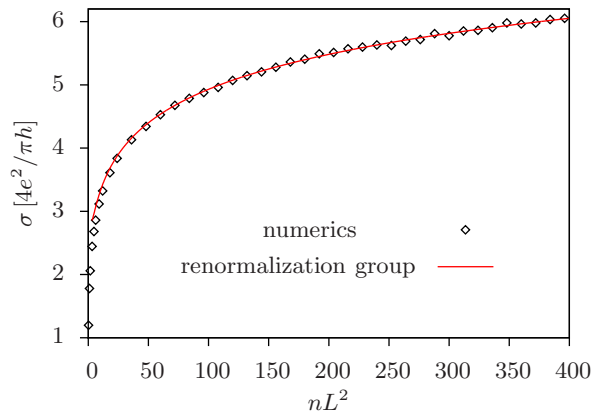


FIG. 1: (Color online) Mean conductivity calculated numerically from Eqs. (12), (14) as a function of concentration of resonance scalar impurities (data points). The data is obtained by interpolation to the limit  $W \gg L$ . The solid line shows the result (16) of the sigma model in class DIII.

For resonant potential impurities, the dependence of the average conductivity  $\sigma = GL/W$  on the impurity concentration  $n = N/LW$  in the limit  $W \gg L$  is plotted in Fig. 1. To understand this behavior analytically, we perform the symmetry analysis of the problem. The matrix  $K$  defined by Eq. (12) yields the Bogoliubov-de-Gennes type of symmetry,  $\sigma_x K^T(-\phi) \sigma_x = -K(\phi)$ , which corresponds to the symmetry class D [25]. The symmetry of the matrix  $K$  is equivalent to that of the transfer matrix of the system and can be used to infer the symmetry class of the corresponding Hamiltonian, which is given by DIII in the present case. The renormalization group analysis of the corresponding sigma model in the two-loop approximation yields the following equation for the dimensionless conductivity [26]

$$\frac{d\bar{\sigma}}{d \ln L} = \frac{2}{\pi} \left( 1 - \frac{1}{\pi \bar{\sigma}} + \mathcal{O}(\bar{\sigma}^{-2}) \right); \quad \bar{\sigma} \equiv \frac{h}{4e^2} \sigma, \quad (15)$$

which holds for  $\bar{\sigma} \gg 1$ , i.e., in the diffusive regime. Solving Eq. (15), we get

$$\sigma = (4e^2/\pi h) (\ln nL^2 - \ln \ln nL^2). \quad (16)$$

Figure 1 shows a perfect agreement between the numerical and analytical results.

An altogether different behavior of the conductivity is obtained from Eqs. (13), (14) for graphene with vacancies. The result is plotted in Fig. 2 in the limit  $W \gg L$  for different relative concentrations,  $n_B/n_A = 0, 1/2, 3/4, 1$ , where  $n_A$  and  $n_B$  stand for the vacancy concentrations in the sublattice A and B, respectively. We see that the conductivity acquires a constant value for  $nL^2 \rightarrow \infty$ . To understand this behavior, we note that the matrix  $K$  from Eq. (13) now possesses the only symmetry  $K^T = K$  and thus belongs to the symmetry class AI. Therefore, graphene with randomly distributed vacancies falls into

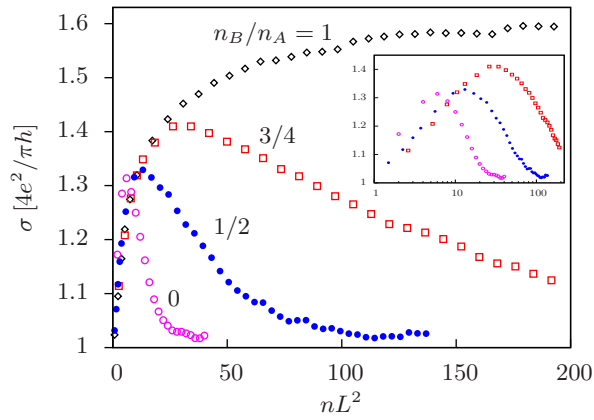


FIG. 2: (Color online) Mean conductivity vs. vacancy concentration,  $n = n_A + n_B$ , found numerically from Eqs. (14), (13) for  $n_B/n_A = 0, 0.5, 0.75, 1$ . Inset illustrates the conductivity scaling for  $n_A \neq n_B$  on the logarithmic scale.

the Hamiltonian symmetry class BDI. The corresponding sigma model is characterized by a vanishing  $\beta$ -function, implying a constant (in general, nonuniversal) value of conductivity in the infrared limit. This is fully consistent with the numerical results of Fig. 2. Remarkably, for  $n_A \neq n_B$ , the conductivity is a non-monotonic function of  $nL^2$  and the limiting value is very close to the  $4e^2/\pi h$ . For equal concentrations,  $n_A = n_B$ , the numerically obtained limiting value is  $\sigma^* \simeq 1.6 \times 4e^2/\pi h$ . The system is expected to show various aspects of criticality characteristic for 2D problem of chiral classes [25].

*Additional comments:* (i) If a small concentration of vacancies is added to the sample with resonant potential impurities, a crossover from DIII behavior, Eq. (16), to BDI (saturation) occurs at some high value of  $\bar{\sigma}$ . (ii) We assumed that the inter-impurity distance is much larger than the graphene lattice constant  $a$ . For very large concentration of potential impurities they will start to overlap and will lose the resonant character. As to vacancies, when their concentration will increase towards  $\sim 1/a^2$ , the conductivity will start to drop, and eventually the system will undergo a localization transition.

In conclusion, we have developed a theoretical approach to transport in disordered systems which describes an entire crossover from ballistic to diffusive or critical regime. The theory can be applied to study localization physics and criticality in a variety of different systems. We have used the theory to calculate the conductivity (and, more generally, the full counting statistics) in undoped graphene with resonant impurities. The conductivity increases logarithmically in the case of smooth resonant potential scatterers (symmetry class DIII) and saturates at a constant value for vacancies (class BDI). In the latter case, the behavior of conductivity depends on the vacancy distribution among two sublattices.

We are grateful to F. Evers, E. Prada, P. San-Jose, and A. Shytov for stimulating discussions. The work was

supported by Rosnauka grant 02.740.11.5072 and by the EUROHORCS/ESF EURYI Award (I.V.G.).

- 
- [1] K. S. Novoselov *et al.*, Science **306**, 666 (2004).
  - [2] K. S. Novoselov *et al.*, Nature (London) **438**, 197 (2005); Y. Zhang *et al.*, Nature (London) **438**, 201 (2005); Y.-W. Tan *et al.*, Eur. Phys. J. Spec. Top. **148**, 15 (2007).
  - [3] A. H. Castro Neto *et al.*, Rev. Mod. Phys. **81**, 109 (2009).
  - [4] M. I. Katsnelson, Eur. Phys. J. B **51**, 157 (2006).
  - [5] J. Tworzydło *et al.*, Phys. Rev. Lett. **96**, 246802 (2006); C. W. J. Beenakker, Rev. Mod. Phys. **80**, 1337 (2008).
  - [6] H. B. Heersche *et al.*, Nature **446**, 56 (2007).
  - [7] F. Miao, *et al.*, Science **317**, 1530 (2007).
  - [8] R. Danneau *et al.*, Phys. Rev. Lett. **100**, 196802 (2008).
  - [9] K. I. Bolotin *et al.*, Solid State Commun. **146**, 351 (2008).
  - [10] Xu Du, I. Skachko, and E. Y. Andrei, Int. J. Mod. Phys. B **22**, 4579 (2008).
  - [11] M. Titov, Europhys. Lett. **79**, 17004 (2007).
  - [12] J. H. Bardarson, *et al.*, Phys. Rev. Lett. **99**, 106801 (2007); K. Nomura, M. Koshino, and S. Ryu, *ibid.* **99**, 146806 (2007); P. San-Jose, E. Prada, and D. S. Golubev, Phys. Rev. B **76**, 195445 (2007); C. H. Lewenkopf, E. R. Mucciolo, and A. H. Castro Neto, *ibid.* **77**, 081410R (2008); J. Tworzydło, C. W. Groth, and C. W. J. Beenakker, *ibid.* **78**, 235438 (2008).
  - [13] A. Schuessler *et al.*, Rev. B **79**, 075405 (2009).
  - [14] Y.-W. Tan, Y. Zhang, H. L. Stormer, and P. Kim, Eur. Phys. J. Special Topics, **148**, 15 (2007).
  - [15] P. M. Ostrovsky, I. V. Gornyi, and A. D. Mirlin, Phys. Rev. B **74**, 235443 (2006).
  - [16] P. M. Ostrovsky, I. V. Gornyi, and A. D. Mirlin, Phys. Rev. Lett. **98**, 256801 (2007).
  - [17] P. M. Ostrovsky, I. V. Gornyi, and A. D. Mirlin, Eur. Phys. J. Spec. Top. **148**, 63 (2007).
  - [18] T. O. Wehling *et al.*, Phys. Rev. B **75**, 125425 (2007); *ibid.*, B **80**, 085428 (2009).
  - [19] T. Stauber, N. M. R. Peres, and F. Guinea, Phys. Rev. B **76**, 205423 (2007).
  - [20] D. C. Elias *et al.* Science **323**, 610 (2009).
  - [21] Z. H. Ni *et al.*, arXiv:1003.0202.
  - [22] J. Bardarson, M. Titov, and P. W. Brouwer, Phys. Rev. Lett. **102**, 226803 (2009).
  - [23] M. Titov *et al.*, Phys. Rev. Lett. **104**, 076802 (2010).
  - [24] S. Ryu *et al.*, Phys. Rev. B **75**, 205344 (2007).
  - [25] for review see F. Evers and A. D. Mirlin, Rev. Mod. Phys. **80**, 1355 (2008).
  - [26] In fact, the sigma model contains an additional Wess-Zumino term (in analogy with  $\mathbb{Z}_2$  topological term in class AII for non-resonant potential scatterers [16]). However, it does not affect the two-loop  $\beta$ -function at large  $\bar{\sigma}$  (15) and thus the asymptotic behavior of conductivity (16). The  $\beta$ -function has a zero at  $\bar{\sigma} = 1/\pi$  corresponding to the Wess-Zumino-Witten fixed point. A remarkable property of class DIII is that this fixed point is unstable:  $\bar{\sigma}$  larger than  $1/\pi$  flows to infinity.
  - [27] Yu. V. Nazarov, Phys. Rev. Lett. **73**, 134 (1994).
  - [28] M. Hentschel and F. Guinea, Phys. Rev. B **76**, 115407 (2007); D. S. Novikov, Phys. Rev. B **76**, 245435 (2007); D. M. Basko, Phys. Rev. B **78**, 115432 (2008).